Physical clustering of *FLC* alleles during Polycomb-mediated epigenetic silencing in vernalization

Stefanie Rosa,[1,5] Filomena De Lucia,[1,5,6] Joshua S. Mylne,[1,2,5,7] Danling Zhu,[1,5] Nobuko Ohmido,[3] Ali Pendle,[1] Naohiro Kato,[4] Peter Shaw,[1] and Caroline Dean[1,8]

[1]Department of Cell and Developmental Biology, John Innes Centre, Norwich Research Park, Norwich NR4 7UH, United Kingdom; [2]The University of Queensland, Institute for Molecular Bioscience, Brisbane, Queensland 4072, Australia; [3]Graduate School of Human Development and Environment, Kobe University, Kobe 657-8501, Japan; [4]Department of Biological Sciences, Louisiana State University, Baton Rouge, Louisiana 70803, USA

Vernalization, the promotion of flowering by cold, involves Polycomb-mediated epigenetic silencing of *FLOWERING LOCUS C* (*FLC*). Cold progressively promotes cell-autonomous switching to a silenced state. Here, we used live-cell imaging of *FLC-lacO* to monitor changes in nuclear organization during vernalization. *FLC-lacO* alleles physically cluster during the cold and generally remain so after plants are returned to warm. Clustering is dependent on the Polycomb *trans*-factors necessary for establishment of the *FLC* silenced state but not on LIKE HETEROCHROMATIN PROTEIN 1, which functions to maintain silencing. These data support the view that physical clustering may be a common feature of Polycomb-mediated epigenetic switching mechanisms.

Supplemental material is available for this article.

Received May 9, 2013; revised version accepted August 12, 2013.

The ability of plants to sense environmental cues and adapt their growth and development accordingly is key to ensuring their reproductive success. One example of this is vernalization, the process by which flowering is accelerated by prolonged cold. A vernalization requirement aligns reproductive development with the favorable conditions of spring. Vernalization in *Arabidopsis thaliana* (*Arabidopsis*) involves the cold-induced epigenetic silencing of FLOWERING LOCUS C (FLC), a MADS box protein that represses flowering (Michaels and Amasino 1999; Sheldon et al. 1999).

Our current understanding of vernalization has been derived from forward genetics combined with chromatin analysis. A well-defined sequence of events has been described (Supplemental Fig. S1) that involves Polycomb-repressive complex 2 (PRC2) and a set of plant homeodomain (PHD) proteins (Gendall et al. 2001; Sung and Amasino 2004; Wood et al. 2006; Greb et al. 2007). An early step in vernalization is disruption of a gene loop (Crevillen et al. 2013), and this is coincident with increased expression of a set of *FLC* antisense transcripts capable of cold-induced down-regulation of linked coding sequences (Swiezewski et al. 2009). These steps precede and are independent of formation of a modified PHD–PRC2 that accumulates at a specific site in *FLC*, covering exon 1 and the beginning of the first intron (Finnegan and Dennis 2007; Angel et al. 2011). The PHD–PRC2 is composed of the canonical PRC2 components including VERNALIZATION2 (VRN2), a Su(Z)12 homolog (Gendall et al. 2001), together with PHD proteins VRN5, VEL1, and the cold-induced VIN3 (Sung and Amasino 2004; Wood et al. 2006; De Lucia et al. 2008). It results in progressive accumulation of H3K27me3 at the nucleation site with increasing cold exposure (Angel et al. 2011). A cold-induced noncoding sense RNA, COLDAIR, aids PRC2 recruitment (Heo and Sung 2011). After plants are transferred back to warm conditions, the PHD–PRC2 (now without VIN3) spreads across the whole gene, causing increased H3K27me3 over the whole locus. The levels of the H3K27me3 again quantitatively reflect the length of cold exposure. This quantitative increase has been shown to reflect a population average of an increasing proportion of cells that have switched to the epigenetically silent state (Angel et al. 2011). Maintenance of this silenced state requires LIKE HETEROCHROMATIN PROTEIN 1 (LHP1) (Mylne et al. 2006; Sung et al. 2006).

An emerging theme in gene regulation is the importance of physical position in the nucleus (Fraser and Bickmore 2007; Bickmore and van Steensel 2013; Hubner et al. 2013). In situ hybridization techniques initially revealed the importance of higher-order sequence interactions and nuclear domains in X-chromosome inactivation (Pollex and Heard 2012), heterochromatin formation, and Polycomb silencing (Brown et al. 1997; Lanzuolo et al. 2007; Bantignies and Cavalli 2011). This understanding has been augmented by chromatin conformation capture techniques that have provided high-resolution interaction maps identifying topologically distinct domains within chromosomes (Noordermeer et al. 2011; Naumova et al. 2012; Shen et al. 2012). Association of changes in gene regulation with alteration of these higher-order structures has been shown for Polycomb silenced loci in *Drosophila* and *Hox* plus X-linked loci in mammals (Lanzuolo et al. 2007; Noordermeer et al. 2011; Nora et al. 2012; Towbin et al. 2012). Live-cell imaging has also revealed the dynamic nature of this nuclear organization, with short- and long-range motion of Polycomb bodies likely to correspond to movement within and between chromosome territories (Hubner and Spector 2010; Matzke et al. 2010; Cheutin and Cavalli 2012).

[*Keywords*: nuclear organization; epigenetic; *FLC*; vernalization; Polycomb]
[5]These authors contributed equally to this work.
Present addresses: [6]Unité de Biologie des Interactions Cellulaires URA CNRS 2582, Institut Pasteur 25, rue du Docteur Roux 75724 Paris Cedex 15, France. [7]School of Chemistry and Biochemistry, ARC Centre of Excellence in Plant Energy Biology, The University of Western Australia, Crawley, Perth, Western Australia 6009, Australia.
[8]Corresponding author
E-mail caroline.dean@jic.ac.uk
Article is online at http://www.genesdev.org/cgi/doi/10.1101/gad.221713.113. Freely available online through the *Genes & Development* Open Access option.

How this dynamic nuclear organization interconnects with specific chromatin changes at individual loci is poorly understood. Here, we used live imaging of a transgene containing a *FLC-lacO* array to monitor nuclear organization and dynamics of *FLC* during vernalization in *Arabidopsis*. This revealed a cold-induced physical clustering of *FLC-lacO* alleles, with the number of cells showing this condition increasing quantitatively with exposure to cold. The clustering is generally stable after cold exposure and is differentially disrupted by the *trans*-factors required for vernalization. These data suggest that physical clustering of *FLC* alleles during the cold phase is an important component of *FLC* epigenetic silencing and support the view that formation of higher-order structures may be an integral component of epigenetic switching mechanisms.

Results and Discussion

Visualization of a functional FLC-lacO transgene in root cells

We wanted to explore the role of nuclear organization during the Polycomb-mediated epigenetic silencing of *FLC* that occurs during vernalization. The goal was to exploit the well-defined sequence of events established for vernalization in order to associate changes in nuclear organization with functionally important steps in Polycomb silencing. An array of 120 copies of the *lacO* DNA sequence—each copy separated by a random ~10-base-pair (bp) sequence to minimize recombinational and replication instability, thus minimizing repeat-induced silencing (Fig. 1A; Lau et al. 2003)—was inserted into the *FLC* gene either downstream from the poly(A) site (Fig. 1A; Supplemental Fig. S2) or into the first intron (Fig. 2K; Supplemental Fig. S2). A *lacO* alone was also generated as a control (Supplemental Fig. S2). Only the *FLC-lacO* construct carrying the *lacO* array downstream from the poly(A) site was fully functional in planta (Supplemental Fig. S3). Three *FLC-lacO* transgenic lines (lines 1, 2, and 3) containing single and complete T-DNA insertions of this construct were then selected (Supplemental Figs. S4, S5). A separate *Arabidopsis* line was generated expressing a LacI-YFP-NLS fusion, and this was crossed with the *lacO* plants. The LacI-YFP-NLS fusion was expressed from the ethanol-inducible promoter (Roslan et al. 2001). *lacO*/*LacI* foci were monitored in root epidermal cells, as these are easily imaged, strongly express *FLC*, and show cold-induced epigenetic silencing of *FLC*. Indeed, vernalized root cells maintain *FLC* silencing even through regeneration into a new plant (Burn et al. 1993). In many experiments, the ethanol-inducible promoter resulted in YFP expression that was too strong to visualize any *lacO* foci, but in the absence of induction, LacI-YFP expression was at an appropriate level in the differentiation zone above the root meristem (Fig. 1B). In this region, cells undergo chromosome endoreduplication, resulting in larger nuclei with higher ploidy (Galbraith et al. 1991). In non-vernalized plants, multiple (six or more) *FLC-lacO* foci were detected in this region of the root (Fig. 1C–F). Careful titration of the ethanol exposure enabled meristematic cells to be imaged, and in these cells, only two foci were detected (Fig. 1G,H). These foci did not associate with an obvious location in the nucleus, sometimes being found at one pole in the nucleus of the elongating cells, sometimes in the center.

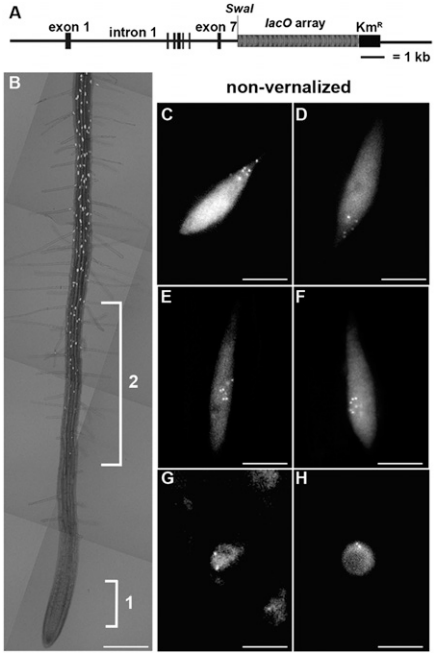

Figure 1. Monitoring *FLC* in root nuclei using an *FLC-lacO* transgene. (*A*) The *lacO* array was inserted downstream from the polyadenylation site of *FLC*. (*B*) *Arabidopsis* root showing expression of LacI-YFP in nuclei predominantly in the differentiation zone (bar, 100 μm). (*C–F*) Representative fluorescence images of nuclei from region 2 showing multiple *FLC* foci. (*G,H*) Representative fluorescence images of nuclei from meristematic cells (from region 1) (bars, 5 μm).

Clustering of FLC-lacO is induced by cold

After the plants had been exposed for 2 wk to 5°C, a large proportion of nuclei showed *FLC-LacO* loci that had clustered into one or two foci in endoreduplicated cells (Fig. 2A–D,G) and one in the meristematic cells (Fig. 2E,F). The foci were larger than those in non-cold-treated plants, consistent with a physical clustering (Supplemental Fig. S6Q,R), and again showed no obvious preferential localization in the nucleus. This clustering was found in all of the independent *FLC-lacO* lines (Supplemental Fig. S6A–P) but was not observed in an *Arabidopsis* line carrying a single and complete *lacO*-only transgene (Fig. 2H–J). The noncomplementing *FLC-lacO* transgene carrying the *lacO* array in the first intron of *FLC* (*FLC-lacO-Bst*) (Fig. 2K–N) also did not show clustering. No RNA was detected from this transgene (Supplemental Fig. S7), suggesting that the clustering process requires expression of the *FLC* gene.

The clustering of FLC-lacO is impaired in vrn2 and vrn5 but not in lhp1

To investigate factors required for clustering, we crossed the *FLC-lacO* line 1 containing the LacI-YFP into different mutant backgrounds (*vrn2*, *vrn5*, and *lhp1*). These mutations impair different phases of the epigenetic silencing of *FLC*; *vrn2* disrupts *FLC* silencing before and during the cold (Gendall et al. 2001), *vrn5* disrupts the accumulation of the silencing in the cold (Greb et al. 2007), and *lhp1* disrupts the maintenance of silencing after the cold (Mylne et al. 2006; Sung et al. 2006). There

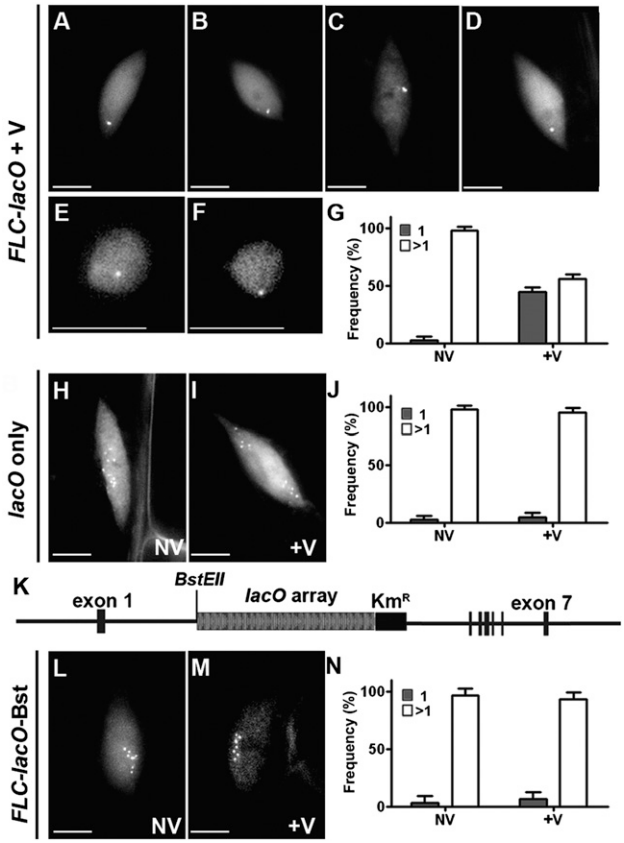

Figure 2. Cold-induced clustering of *FLC-lacO*. (*A–D*) Representative fluorescence images of *Arabidopsis* root cells (from region 2) (see Fig. 1B) in plants grown in cold for 2 wk (and imaged immediately afterward) showing clustering of *FLC-lacO* loci. (*E,F*) Clustering of *FLC-lacO* copies in meristematic cells in plants cold-treated for 2 wk. LacI-YFP expression was induced using a 1% ethanol vapor treatment for 1.5 h. (*G*) Quantification of the *FLC-lacO* foci (30 cells counted in three different roots) from cells in region 2. (*H,I*) Representative fluorescence images of nuclei from cells in region 2 expressing a *lacO*-only transgene. Plants were either nonvernalized (NV) or vernalized for 2 wk (+V). (*J*) Quantification of the *lacO* foci (30 cells counted in three different roots) from cells in region 2. (*K*) *FLC-lacO* transgene with the *lacO* array inserted at the BstEII restriction site in *FLC* intron 1 of the genomic *FLC* sequence. (*L,M*) Representative fluorescence images of *FLC-lacO-Bst* transgene in root cells from region 2 nonvernalized (*L*) and vernalized for 2 wk (*M*). (*N*) Quantification of the *FLC-lacO-Bst* foci from cells in region 2 (30 cells counted in three different roots) nonvernalized and vernalized for 2 wk (bars, 5 μm).

was a slightly higher level of preclustering in the *vrn5* mutant compared with *vrn2*, but both abolished the cold-induced clustering of the *FLC-lacO* foci in the root epidermal cells (Fig. 3A–D,G,H). In contrast, the cold-induced clustering at the end of the cold, or shortly after return to the warm, occurred normally in the *lhp1* mutant (Fig. 3E,F). These data suggest that physical clustering of the *FLC-lacO* alleles in the cold requires the same components as the PHD–PRC2 nucleation event rather than those functioning later in the vernalization process.

The clustering of FLC-lacO increases quantitatively with increasing cold exposure

We next considered how the timing of changes in cold-induced physical clustering compared with other cold-induced processes involved in vernalization. The robust gene loop that is found in many genotypes in warm-grown plants is disrupted in the first few weeks of cold exposure (Crevillen et al. 2013), increased antisense transcription is maximal after 2–3 wk of exposure (Swiezewski et al. 2009), and the increase in H3K27me3 at the nucleation site occurs quantitatively throughout the first 4 wk of cold (Angel et al. 2011). To compare the dynamics of cold-induced clustering with the timing of these other cold-induced steps, the number of cells showing reduced numbers of *FLC-lacO* foci was measured in plants exposed to different lengths of cold (Fig. 4A; Supplemental Fig. S8). The time-dependent increase in clustering during the cold paralleled the increase in H3K27me3 at the intronic nucleation site (Fig. 4E). Previous work combining modeling and experimental analysis revealed that the quantitative increase in epigenetic silencing, so characteristic of vernalization, is the result of a cell-autonomous switching mechanism, with the probability of switching increasing with increasing exposure to cold (Angel et al. 2011). The parallels observed in this study between clustering and H3K27me3 nucleation suggest that this cell-autonomous switching mechanism might involve the

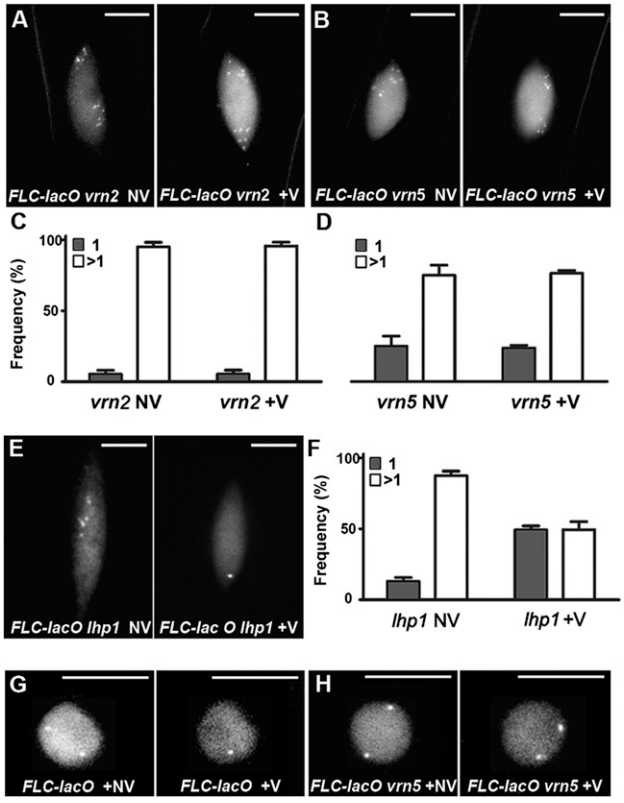

Figure 3. The clustering of *FLC-lacO* is impaired in *vrn2* and *vrn5* but not in *lhp1*. (*A*) Region 2 root cells either nonvernalized (NV) or vernalized for 2 wk (+V). (*B*) *vrn5* nonvernalized (NV) or vernalized for 2 wk (+V). (*C*) Quantification of *FLC-lacO* foci in 30 *vrn2* cells in region 2. (*D*) Quantification of *FLC-lacO* foci in 30 *vrn5* cells in region 2. (*E*) Images of *FLC-lacO* transgene in *lhp1* background nonvernalized (NV) or vernalized for 2 wk (+V). (*F*) Quantification of *FLC-lacO* foci in 50 *lhp1* cells in region 2. (*G,H*) Representative fluorescence images of nuclei from meristematic cells harboring the *FLC-lacO* from plants nonvernalized (NV) or vernalized for 2 wk (+V) in wild type (*G*) and *vrn5* (*H*) (bars, 5 μm).

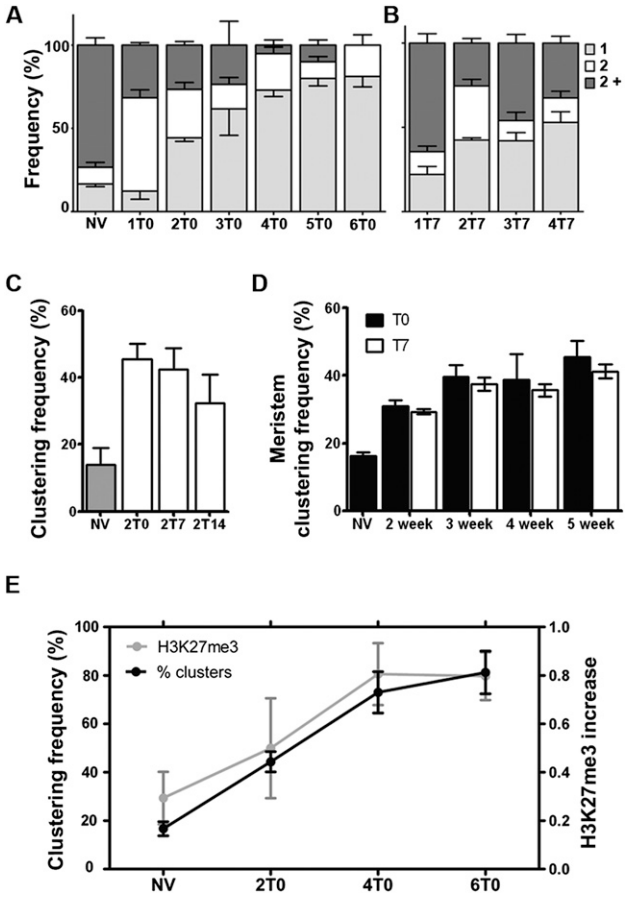

Figure 4. The clustering of *FLC-lacO* increases quantitatively with increasing cold exposure. (*A*) Time course of *FLC-lacO* clustering after different weeks of cold (XT0). The number of foci (one, two, or more than two) was counted in 10 randomly selected nuclei in five different plants. (*B*) The same analysis but after cold the plants were grown for 7 d (T7) at 20°C before imaging. The number of foci (one, two, or more than two) was counted in 10 randomly selected nuclei in five different plants. (*C*) Quantification of the proportion of cells in region 2 showing one *FLC-lacO* cluster after 2 wk of cold and at post-cold time points T7 (7 d post-transfer from cold) and T14. (*D*) Quantification of cells in the meristematic region showing one *FLC-lacO* cluster. *FLC-lacO* clustering in the meristem was quantified in nonvernalized (NV) plants and plants vernalized for different lengths (2–5 wk) as well as at the respective T7 time point. For this analysis, at least three different plants were used for quantification at each time point. (*E*) Clustering dynamics parallel the cold-induced increases in H3K27me3 at the nucleation site. With increasing cold exposure, H3K27me3 levels increase at the nucleation site (end of exon 1–start intron 1), the timing of which is coincident with the reduction in *FLC-lacO* foci number. *FLC* is fully silenced after 6 wk of cold, and this is associated with high H3K27me3 and maintenance of the clustering during subsequent growth at warm temperatures. Gray data points represent the increase of H3K27me3 at the nucleation site normalized to H3 and *SHOOT MERISTEMLESS* (data from Angel et al. 2011). Black data points represent the frequency of one *FLC–lacO* cluster.

switch of physical position of the *FLC* locus in the nucleus.

We then investigated whether the cold-induced clustering was maintained through subsequent cell division after plants were returned to warm conditions. Analysis of endoreduplicated and meristematic cells showed that clustering was generally maintained for 7 d after transfer from the cold (Fig. 4B–D). However, the endoreduplicated cells tended to lose clustering (Fig. 4B,C) slightly more than cells in the meristem (Fig. 4D). We attempted to ask whether the clustering was associated with formation of structures equivalent to Polycomb bodies in mammals (Bantignies and Cavalli 2011) by colocalization of LacI-YFP, *FLC-lacO*, and VRN2 using immunofluorescence, but the local concentration of the LacI-YFP protein proved too low to detect the *FLC-lacO* foci using anti-YFP/GFP antibodies. We were also unable to analyze colocalization of *FLC-lacO* with other Polycomb targets, as clustering was not observed after the extensive fixation and hybridization procedures required for in situ hybridization in plant cells (Supplemental Fig. S9). We interpret this as suggesting that, as in other organisms, the clusters involved in the Polycomb silencing underlying vernalization are highly dynamic structures (Hubner and Spector 2010; Matzke et al. 2010; Cheutin and Cavalli 2012). There is also the possibility that the *FLC-lacO* repeats stabilize more transient interactions of the endogenous loci.

Our demonstration of cold-induced clustering of *FLC-lacO* alleles during vernalization suggests that physical repositioning in the nucleus may be a common feature of Polycomb-mediated epigenetic silencing. Robustness in regulatory mechanisms generally involves feedback loops, so we envisage that some aspect of silencing results in clustering, but that clustering then reinforces the silencing. The clustering may be one manifestation of the cell-autonomous switching mechanism proposed for vernalization, and it is an attractive model to generally account for localization of silenced chromosomal domains into Polycomb bodies. Interconnecting the different aspects of these silencing mechanisms will be crucial to fully understand how they reinforce each other, ensuring mitotic inheritance of epigenetic regulation.

Materials and methods

Constructs and transgenic lines

Three constructs were used in this study: a *FLC* reporting construct containing genomic *FLC* with a *lacO* array and kanamycin resistance cassette inserted at either the SwaI site downstream from the *FLC* poly(A) site (*FLC-lacO*) or the BstEII site within the first intron (*FLC-lacO-Bst*) and a control containing only the *lacO* array and kanamycin resistance cassette (*lacO* only). To produce the *FLC* reporting construct (*FLC-lacO*), a 12-kb SacI fragment of Columbia genomic DNA was cloned in pBS (pFLC15), including 3.7 kb upstream of the *FLC* start ATG to 2.7 kb downstream from the end of the *FLC* 3′ untranslated region (UTR). The *lacO* array was obtained from the vector pLAU41, which contains ~120 copies of the *lacO* DNA sequence, each interspersed with random ~10-mers and a kanamycin resistance (Km^R) cassette within a pUC18 backbone similar to the published vector pLAU43. This interspersed repeat array reduced problems with repeat-induced silencing (Lau et al. 2003). To produce the *FLC* construct with the *lacO* array in the first intron (*FLC-lacO-Bst*), an approach similar to *FLC-lacO* was used, but instead the 5.3-kb *lacO-Km*^{R} fragment was inserted at the BstEII site. The control contained only the *lacO* array and kanamycin resistance cassette (*lacO* only).

The constructs were cloned into *Agrobacterium* binary vector pSLJ755I5 and transformed into *flc-3* FRI^{SF2} containing a small deletion at the 5′ end of *FLC* and an active *FRIGIDA* allele from the *Arabidopsis* accession San-Feliu-2 (Michaels and Amasino 2001). The BstEII *lacO*-containing *FLC* constructs did not delay the flowering time of *flc-3* FRI^{SF2} at all and therefore were deemed nonfunctional.

Fluorescent in situ hybridization

Arabidopsis roots were fixed for 60 min with 4% (w/v) formaldehyde freshly made from paraformaldehyde (PFA) in PBS buffer. After washing in PBS for 5 min, the roots were digested in a mixture of 1% driselase, 0.5% cellulase, and 0.025% pectolyase for 45–60 min at 37°C. After enzyme treatment, roots were washed in PBS three times for 5 min each and squashed between poly-L lysine slides (Polysine, VWR International) and coverslips in PBS. After the slides were frozen in liquid nitrogen, the coverslips were removed, and the samples were air-dried. Slides were treated with 10 mg/mL RNase for 1 h at 37°C and washed twice in 2× SSC. Probes were labeled with Cy3-dUTP (Sigma) by nick translation. Bacterial artificial chromosome (BAC) clone JAtY79P05, which contains an insert of 60.12 kb, was used as a probe for the native *Arabidopsis* genome immediately adjacent to the *FLC-lacO* T-DNA on the bottom arm of chromosome V ("BAC probe") or the 5.3 kb of the *lacO* array ("*lacO* probe"). The hybridization mixture (20 ng/μL labeled DNA, 50% formamide, 10% dextran sulfate, 2× SSC) was applied to the slides, which were then denatured for 7 min at 75°C, 3 min at 55°C, min, and 3 min at 50°C and hybridized overnight at 37°C. After hybridization, slides were washed at 42°C once in 2× SSC, twice in 20% formamide 2× SSC, and twice in 2× SSC and then at room temperature twice in 2× SSC and twice in 4× SSC and 0.1% Tween 20. Nuclei were counterstained with 1 μg/mL DAPI (4′,6-diamidino-2-phenylindole dihydrochloride hydrate; Sigma), and slides were mounted in Vectashield (Vector Laboratories). RNA in situ hybridization was performed on nonvernalized and 4-wk vernalized wild-type and *FLC-lacO* seedling roots.

Live imaging

Arabidopsis seedlings were placed in a biochamber constructed from a standard coverslip, a well (~16 × 24 mm) made in Secure Seal (double-sided adhesive sheet; Grace Bio-Labs) filled with MS medium, and a gas-permeable membrane (BioFolie, Viva Science) attached to the Secure Seal as the bottom of the chamber. The chamber with the gas-permeable membrane facing down was then placed over a 1-cm hole drilled into a plastic support slide to allow free gaseous exchange through the gas-permeable membrane, and the edges of the sandwich were sealed with tape.

Imaging was performed using a 60× oil lens on a Nikon Eclipse 600 epifluorescence microscope equipped with a Hamamatsu Orca ER cooled CCD digital camera and a Prior Proscan *x*–*z* stage. The following wavelengths were used for fluorescence detection: excitation 340–380 nm and emission 425–475 nm for DAPI, and excitation 490–510 nm and emission 520–550 nm for YFP. For all experiments, series of optical sections with *z*-steps of 150 or 200 nm were collected using MetaMorph software (Universal Imaging). The images from *z* sections were projected using the maximum intensity projection algorithm in the ImageJ program.

Acknowledgments

We thank Kim Johnson for help with TAIL-PCR, and Maike Stam, Robert Sablowski, Silvia Costa, and Clive Lloyd for comments on the manuscript. F.D.L. was supported by Biotechnology and Biological Sciences Research Council (BBSRC) grant BB/C517633/1 and European Research Council grant 233039 ENVGENE. S.R. was supported by grant SFRH/BD/23202/2005 from the Portuguese Fundação para a Ciência e a Tecnologia. J.S.M. was supported by European Commission grant QLK5-CT-2001-01412, an ARC QEII Fellowship (DP0879133), and an ARC Future Fellowship (FT120100013). P.S. and C.D. acknowledge support from ISP grant BB/J004588/1 from the BBSRC and the John Innes Foundation.

References

Angel A, Song J, Dean C, Howard M. 2011. A Polycomb-based switch underlying quantitative epigenetic memory. *Nature* **476:** 105–108.

Bantignies F, Cavalli G. 2011. Polycomb group proteins: Repression in 3D. *Trends Genet* **27:** 454–464.

Bickmore WA, van Steensel B. 2013. Genome architecture: Domain organization of interphase chromosomes. *Cell* **152:** 1270–1284.

Brown KE, Guest SS, Smale ST, Hahm K, Merkenschlager M, Fisher AG. 1997. Association of transcriptionally silent genes with Ikaros complexes at centromeric heterochromatin. *Cell* **91:** 845–854.

Burn JE, Bagnall DJ, Metzger JD, Dennis ES, Peacock WJ. 1993. DNA methylation, vernalization, and the initiation of flowering. *Proc Natl Acad Sci* **90:** 287–291.

Cheutin T, Cavalli G. 2012. Progressive polycomb assembly on H3K27me3 compartments generates polycomb bodies with developmentally regulated motion. *PLoS Genet* **8:** e1002465.

Crevillen P, Sonmez C, Wu Z, Dean C. 2013. A gene loop containing the floral repressor *FLC* is disrupted in the early phase of vernalization. *EMBO J* **32:** 140–148.

De Lucia F, Crevillen P, Jones AM, Greb T, Dean C. 2008. A PHD–polycomb repressive complex 2 triggers the epigenetic silencing of *FLC* during vernalization. *Proc Natl Acad Sci* **105:** 16831–16836.

Finnegan EJ, Dennis ES. 2007. Vernalization-induced trimethylation of histone H3 lysine 27 at FLC is not maintained in mitotically quiescent cells. *Curr Biol* **17:** 1978–1983.

Fraser P, Bickmore W. 2007. Nuclear organization of the genome and the potential for gene regulation. *Nature* **447:** 413–417.

Galbraith DW, Harkins KR, Knapp S. 1991. Systemic endopolyploidy in *Arabidopsis thaliana*. *Plant Physiol* **96:** 985–989.

Gendall AR, Levy YY, Wilson A, Dean C. 2001. The *VERNALIZATION 2* gene mediates the epigenetic regulation of vernalization in *Arabidopsis*. *Cell* **107:** 525–535.

Greb T, Mylne JS, Crevillen P, Geraldo N, An H, Gendall AR, Dean C. 2007. The PHD finger protein VRN5 functions in the epigenetic silencing of *Arabidopsis FLC*. *Curr Biol* **17:** 73–78.

Heo JB, Sung S. 2011. Vernalization-mediated epigenetic silencing by a long intronic noncoding RNA. *Science* **331:** 76–79.

Hubner MR, Spector DL. 2010. Chromatin dynamics. *Annu Rev Biophys* **39:** 471–489.

Hubner MR, Eckersley-Maslin MA, Spector DL. 2013. Chromatin organization and transcriptional regulation. *Curr Opin Genet Dev* **23:** 89–95.

Lanzuolo C, Roure V, Dekker J, Bantignies F, Orlando V. 2007. Polycomb response elements mediate the formation of chromosome higher-order structures in the bithorax complex. *Nat Cell Biol* **9:** 1167–1174.

Lau IF, Filip SR, Soballe B, Okstad O, Barre F, Sherratt DJ. 2003. Spatial and temporal organization of replicating *Escherichia coli* chromosomes. *Mol Microbiol* **49:** 731–743.

Matzke AJ, Watanabe K, van der Winden J, Naumann U, Matzke M. 2010. High frequency, cell type-specific visualization of fluorescent-tagged genomic sites in interphase and mitotic cells of living *Arabidopsis* plants. *Plant Methods* **6:** 2.

Michaels SD, Amasino RM. 1999. FLOWERING LOCUS C encodes a novel MADS domain protein that acts as a repressor of flowering. *Plant Cell* **11:** 949–956.

Michaels SD, Amasino RM. 2001. Loss of FLOWERING LOCUS C activity eliminates the late-flowering phenotype of FRIGIDA and autonomous pathway mutations but not responsiveness to vernalization. *Plant Cell* **13:** 935–941.

Mylne JS, Barrett L, Tessadori F, Mesnage S, Johnson L, Bernatavichute YV, Jacobsen SE, Fransz P, Dean C. 2006. LHP1, the *Arabidopsis* homologue of HETEROCHROMATIN PROTEIN1, is required for epigenetic silencing of FLC. *Proc Natl Acad Sci* **103:** 5012–5017.

Naumova N, Smith EM, Zhan Y, Dekker J. 2012. Analysis of long-range chromatin interactions using Chromosome Conformation Capture. *Methods* **58:** 192–203.

Noordermeer D, Leleu M, Splinter E, Rougemont J, De Laat W, Duboule D. 2011. The dynamic architecture of Hox gene clusters. *Science* **334:** 222–225.

Nora EP, Lajoie BR, Schulz EG, Giorgetti L, Okamoto I, Servant N, Piolot T, van Berkum NL, Meisig J, Sedat J, et al. 2012. Spatial partitioning of the regulatory landscape of the X-inactivation centre. *Nature* **485:** 381–385.

Pollex T, Heard E. 2012. Recent advances in X-chromosome inactivation research. *Curr Opin Cell Biol* **24:** 825–832.

Roslan HA, Salter MG, Wood CD, White MR, Croft KP, Robson F, Coupland G, Doonan J, Laufs P, Tomsett AB, et al. 2001. Characterization of the ethanol-inducible alc gene-expression system in *Arabidopsis thaliana*. *Plant J* **28:** 225–235.

Sheldon CC, Burn JE, Perez PP, Metzger J, Edwards JA, Peacock WJ, Dennis ES. 1999. The FLF MADS box gene: A repressor of flowering in *Arabidopsis* regulated by vernalization and methylation. *Plant Cell* **11:** 445–458.

Shen Y, Yue F, McCleary DF, Ye Z, Edsall L, Kuan S, Wagner U, Dixon J, Lee L, Lobanenkov VV, et al. 2012. A map of the *cis*-regulatory sequences in the mouse genome. *Nature* **488:** 116–120.

Sung S, Amasino RM. 2004. Vernalization in *Arabidopsis thaliana* is mediated by the PHD finger protein VIN3. *Nature* **427:** 159–164.

Sung S, He Y, Eshoo TW, Tamada Y, Johnson L, Nakahigashi K, Goto K, Jacobsen SE, Amasino RM. 2006. Epigenetic maintenance of the vernalized state in *Arabidopsis thaliana* requires LIKE HETEROCHROMATIN PROTEIN 1. *Nat Genet* **38:** 706–710.

Swiezewski S, Liu F, Magusin A, Dean C. 2009. Cold-induced silencing by long antisense transcripts of an *Arabidopsis* Polycomb target. *Nature* **462:** 799–802.

Towbin BD, Gonzalez-Aguilera C, Sack R, Gaidatzis D, Kalck V, Meister P, Askjaer P, Gasser SM. 2012. Step-wise methylation of histone H3K9 positions heterochromatin at the nuclear periphery. *Cell* **150:** 934–947.

Wood CC, Robertson M, Tanner G, Peacock WJ, Dennis ES, Helliwell CA. 2006. The *Arabidopsis thaliana* vernalization response requires a polycomb-like protein complex that also includes VERNALIZATION INSENSITIVE 3. *Proc Natl Acad Sci* **103:** 14631–14636.